

DESY, February 2001, TESLA Report 2001-04

Concept of the High Power e^\pm Beam Dumps for TESLA

W. Bialowons, M. Maslov, M. Schmitz, V. Sytchev

Concept of the High Power e^\pm Beam Dumps for TESLA

W. Bialowons, M. Maslov, M. Schmitz, V. Sytchev

Table of Contents

| | | |
|-------|---|----|
| 1 | Introduction..... | 2 |
| 2 | Consideration of Candidate Materials for the Beam Dump..... | 2 |
| 3 | Concept of the Graphite based Beam Dump..... | 6 |
| 3.1 | Energy Deposition..... | 8 |
| 3.2 | Slow Sweeping System..... | 9 |
| 3.3 | Thermal and Mechanical Stress Analysis of the Graphite based Solid Dump | 10 |
| 3.4 | Water Cooling..... | 11 |
| 3.5 | Summary of Solid Dump Characteristics | 12 |
| 4 | Concept of the Water based Beam Dump | 13 |
| 4.1 | The Water Absorber..... | 13 |
| 4.1.1 | Energy deposition and energy leakage..... | 13 |
| 4.2 | Water Cooling and Preparation System..... | 15 |
| 4.2.1 | Working temperature and pressure | 16 |
| 4.2.2 | Water radiolysis | 16 |
| 4.2.3 | Radioactivity and water filtering..... | 17 |
| 4.3 | Summary of Water Dump Characteristics | 17 |
| 5 | Conclusion..... | 18 |
| 6 | References..... | 19 |

1 Introduction

The TESLA accelerator is equipped with quite a number of extraction lines and beam dumps. Below we consider the case of the most powerful main dump, placed in the main linac tunnel. Updated beam parameters at 250 GeV operation are specified in Table 1.

The main requirements to the dumps can be summarized as follows:

- 1) The beam dump must absorb 2.256 MJ per macro pulse (bunch train).
- 2) Average absorbed beam power is 11.28 MW.
- 3) Energy absorption efficiency must be more than 99%.
- 4) The dump assembly must be as compact as possible to fit inside the dump hall.
- 5) Production of radioactive isotopes must be minimized.
- 6) The absorbing part of the dump (the dump core) must be designed without expecting any major maintenance or repair work during its full operation period of about 10 to 20 years.

| | TESLA CDR | TESLA TDR |
|--|--------------|----------------|
| length of bunch train t_{pulse} , [ms] | 0.8 | 0.95 |
| bunches per bunch train n_b | 1130 | 2820 |
| bunch spacing, [ns] | 708 | 337 |
| bunch train repetition rate ν , [Hz] | 5 | 5 |
| particles per bunch N_e , [10^{10}] | 3.6 | 2 |
| particles per bunch train $N_t = N_e \cdot n_b$, [10^{13}] | 4.068 | 5.64 |
| average beam current $I_{\text{ave}} = e \cdot N_t \cdot \nu$, [μA] | 32.544 | 45.12 |
| beam energy per bunch train, [MJ] | 1.6 | 2.256 |
| average beam power, [MW] | 8 | 11.28 |
| spot size at the dump entrance (undisrupted beam) $\sigma_x \times \sigma_y$, [mm] | 3 x 0.5 | 1 x 0.4 |

Table 1: Updated TESLA 500 parameters valid for the TDR, compared with those in the CDR

In order to design a beam dump, which allows reliable long term operation, different candidate materials are evaluated. Two principally different beam dump concepts and their technical realization are investigated in this paper. The first concept uses a solid beam dump based on a graphite core, while the second approach discusses the water dump scheme. From the comparison of both concepts it will become quite obvious, that at average beam power levels beyond several hundreds of kW, the water based beam dump system is the only reasonable choice.

2 Consideration of Candidate Materials for the Beam Dump

The maximum temperature in a solid dump core can be estimated as a composition from two contributions. Each bunch train causes a certain distribution of deposited energy density in the absorber. Since the time interval t_{pulse} , in which this happens, is

short compared to thermal diffusion processes, the material will experience an instantaneous temperature jump ΔT_{inst} , which decays according to heat conduction until the next one arrives. Therefore the average temperature level will rise by about ΔT_{eq} , which is the solution of the heat equation, assuming a constant and not pulsed heat source, given by the average beam current. Therefore an upper limit T_{max} on the maximum temperature in the solid absorber can be given as the sum of both contributions, which add to the temperature of the heat sink T_{cool} :

$$T_{\text{max}} \approx T_{\text{cool}} + (\Delta T_{\text{inst}})_{\text{max}} + (\Delta T_{\text{eq}})_{\text{max}}$$

The incident particles initiate an electromagnetic shower (EMS) in the dump material, which causes a certain spatial distribution of deposited energy dE/dV . The maximum local energy density per mass unit and per one incident particle $(dE/dm)_{\text{max}}$ depends on the spot size of the incoming beam. Integrating the local energy density dE/dV radially and azimuthally gives the longitudinal energy profile of the shower dE/dz , which does not depend on the incident spot size. Especially for a small beam size the position of the shower maximum with $(dE/dz)_{\text{max}}$ differs from the location of $(dE/dm)_{\text{max}}$. The longitudinal and transversal distribution of an EMS developing in a material, can be characterized by its radiation length X_0 , its critical energy E_c and its Molière radius $R_m = 21.1 \text{MeV} \cdot X_0 / E_c$. For an infinitely long cylindrical absorber with

| | Be | C | Al | Cu | Ti | H ₂ O |
|--|------|------|-----|------|------|------------------|
| $(dE/dm)_{\text{max}}$ [GeV/g/electron] | 2 | 3.4 | 6.5 | 26.7 | 12.7 | 2.3 |
| $(dE/dz)_{\text{max}}$ [GeV/cm/electron] | 0.79 | 1.07 | 2.8 | 16 | 6.5 | 0.72 |
| X_0 [cm] | 35.2 | 25 | 8.9 | 1.43 | 3.56 | 36.3 |
| R_m [cm] | 5.7 | 7 | 4.7 | 1.6 | 2.6 | 9.6 |

Table 2: Main characteristics of an EMS at 250 GeV developing in different materials

radius R_m , about 10% of the incident particle energy leaks radially [2]. Here it is assumed that the absorber is completely enclosed by the same material, thus backscattering into the absorber will contribute. As calculated with the shower simulation code MARS 13 [3], table 2 gives the main characteristics of the EMS for different materials at 250 GeV energy and a spot size of $0.35 \text{mm} \times 0.5 \text{mm}$.

In order to judge, whether the temperatures caused by the EMS are harmful to a given material, one needs to set reasonable allowed limits. For cyclic thermal load such a limit $\Delta T_{\text{max}}^{\text{cyclic}}$ is given by the corresponding cyclic mechanical stress, which should not exceed the endurance limit σ_u of the material. The endurance limit is the stress value that does not produce damage effects in the material after a certain number of cycles (typically 10^7 - 10^8). A reasonable limit of average heating $\Delta T_{\text{max}}^{\text{ave}}$ for the material of interest will be given either by 20% of its melting point T_{melt} or its yield strength $\sigma_{0.2}$, depending on which of both is less [4]. Therefore these limits, being listed together with the main thermal and mechanical parameters [5] for different materials in table 3, can be written as:

$$\Delta T_{\text{max}}^{\text{cyclic}} = \frac{\sigma_u}{2\alpha E} \quad \text{and} \quad \Delta T_{\text{max}}^{\text{ave}} = \text{Min} \left\{ \frac{\sigma_{0.2}}{\alpha E} \quad \text{or} \quad 0.2 \cdot (T_{\text{melt}} - 20^\circ \text{C}) \right\}$$

| | ρ [g/cm ³] | c [J/g/K] | E [GPa] | λ [W/cm/K] | α [10 ⁻⁶ /K] | σ_u (# of cycles) [MPa] | $\Delta T_{\max}^{\text{cyclic}}$ [K] | $\Delta T_{\max}^{\text{ave}}$ [K] |
|------------------|--------------------------------|----------------|--------------|-----------------------|-----------------------------------|--------------------------------------|--|---------------------------------------|
| Be | 1.85 | 2.05 | 300 | 1.6 | 12.4 | 100 (1·10 ⁷) | 15 | 100 |
| Ti | 4.6 | 0.565 | 110 | 0.1 | 8.5 | 530 (1·10 ⁷) | 280 | 300 |
| Al | 2.85 | 0.922 | 70 | 2.0 | 23 | 100 (2·10 ⁷) | 30 | 60 |
| Cu | 8.96 | 0.38 | 120 | 4 | 17 | 28 ¹⁾ | 20 | 100 |
| C | 1.7 | 0.96 | 10 | 0.7 - 1 | 7 | 60 ²⁾ | 400 | 800 |
| H ₂ O | 1 | 4.2 | | | | | 80 – 300 ³⁾ | 80 – 300 ³⁾ |

¹⁾ estimation $\sigma_u = 0.4s_{0.2}$, ²⁾ compression loading, ³⁾ depending on water pressure

Table 3: Thermal and mechanical properties of materials relevant for beam dumps

Where α is the coefficient of linear thermal expansion and E is the elastic modulus of the material.

Maximum instantaneous heating of the dump material within one bunch train passage is determined by $N_t \cdot (dE/dm)_{\max} = c \cdot (\Delta T_{\text{inst}})_{\max}$. For a bunch train population

| | Be | C | Al | Cu | Ti | H ₂ O |
|---|------------------|------------------|------------------|------------------|------------------|------------------|
| $N_t \cdot (dE/dm)_{\max}$ [kJ/g per bunch train] | 18 | 31 | 59 | 240 | 110 | 21 |
| $(\Delta T_{\text{inst}})_{\max}$ [K] | $8.8 \cdot 10^3$ | $3.2 \cdot 10^4$ | $6.5 \cdot 10^4$ | $2.4 \cdot 10^5$ | $1.1 \cdot 10^5$ | $5 \cdot 10^3$ |
| $(\Delta T_{\text{inst}})_{\max} / \Delta T_{\max}^{\text{cyclic}}$ | 610 | 36-50 | 3200 | 30000 | 690 | 25-200 |

Table 4: Instantaneous heating in different materials after passage of a bunch train, with $N_t = 5.64 \cdot 10^{13}$

of $N_t = 5.64 \cdot 10^{13}$ table 4 compares this temperature rise with the tolerable limit $\Delta T_{\max}^{\text{cyclic}}$. From that point of view water and graphite are favourable materials in dump applications. The assumption of instantaneous processes is justified, since during the bunch train passage time of $t_{\text{pulse}} \approx 1\text{ms}$ the temperature distribution propagates by a typical diffusion length of $L = \sqrt{(\lambda \cdot t_{\text{pulse}}) / (\rho \cdot c)}$, where λ is the specific heat conductivity, c the specific heat and ρ the mass density of the material. This value is only ≈ 0.3 mm for copper and graphite. which is smaller than the required beam spot size at the dump entrance as will be seen later.

To estimate the dump heating at equilibrium conditions we consider an infinitely long solid plate of rectangular shape, having a width w and a height of $4R_m$. Water cooling is applied on both flat surfaces. A beam with a size of $\sigma \ll R_m$ is homogeneously distributed across the width of the plate at a line in the middle of the plate height. According to heat conduction considerations the maximum equilibrium temperature rise in this case is:

$$\Delta T_{\text{eq}} = N_t \cdot v \cdot \left(\frac{dE}{dz} \right)_{\text{max}} \cdot \frac{R_m}{w \cdot \lambda} = \left(\frac{dP}{dz} \right)_{\text{max}} \cdot \frac{R_m}{w \cdot \lambda}$$

For different materials table 5 lists the maximum power densities and the required plate width w , in order to achieve sufficient heat conductivity to keep $\Delta T_{\text{eq}} \leq \Delta T_{\text{max}}^{\text{ave}}$.

| | Be | C | Al | Cu | Ti | H ₂ O |
|----------------------------------|----|----|-----|-----|-----|------------------|
| $(dP/dz)_{\text{max}}$, [kW/cm] | 34 | 48 | 126 | 722 | 290 | 32 |
| required w , [m] | 12 | 6 | 49 | 28 | 250 | *) |

*) heat removal from water dump by mass flow of water

Table 5: Maximum average power density and requirements on absorber dimensions to support sufficient heat conduction, 250 GeV beam with $I_{\text{ave}} = 45\mu\text{A}$

The numbers are given for a 250 GeV beam with $I_{\text{ave}} = 45\mu\text{A}$, i.e. 11.3 MW of average beam power. As a consequence the beam has to be distributed along a path of several meters! Even in the case of graphite a slow sweep path length of about 6 m is required. In case of a liquid absorber material, like water, the deposited heat can be removed by water circulation towards an external heat exchanger. From the data given in table 4 and table 5 one can conclude as follows:

- 1) Amongst the solid materials graphite is the best candidate for a beam dump core. A water based dump is considered as an alternative option.
- 2) The heat flux at the shower maximum caused by a 11 MW beam is 48 kW/cm for the graphite beam dump and 32 kW/cm for the water beam dump. To remove this power from the solid dump its heat exchange cross section should be more than 1200 cm² per one cm of dump length. A slow sweeping system has to distribute the incident beam.

Heat removal from the water dump is provided by circulation of the dump water.

- 3) Special measures, like a fast beam sweeping system, should be foreseen to reduce the maximum energy deposition density and related instantaneous temperature jump in the dump during one bunch train passage.

3 Concept of the Graphite based Beam Dump

During the TESLA CDR stage a concept of a solid beam dump has been elaborated. Therefore the following discussion is based on the parameters as had been valid for the CDR. They were already given in the introduction in table 1.

The solid beam dump approach is a sandwich like dump made from graphite sections. Each section consists of 5 graphite layers embedded within water-cooled copper plates. If the copper cooling plates are being hit accidentally, e.g. in case of a failure of the slow beam sweeping system, their temperature can reach a maximum of about 3000 K. Thus a graphite collimator section must be installed upstream of the absorber in order to protect the copper.

The principal scheme of such a beam dump is shown in figure 1. This beam dump consists of the following main components:

- Five graphite sections (of which only 4 are shown in figure 1). Their length is 1.0 m. Cross section is $0.24\text{m} \times 1\text{m}$.
- A $13 X_0$ long copper section is installed at the rear side of the dump (tail catcher).
- Graphite collimator is installed in front of the dump.
- Noble gas filled dump container to avoid graphite oxidation and air activation.
- Water-cooled copper heat sinks embedded within the graphite section.
- Support steel structure.
- Huge entrance window to allow slow beam sweeping.

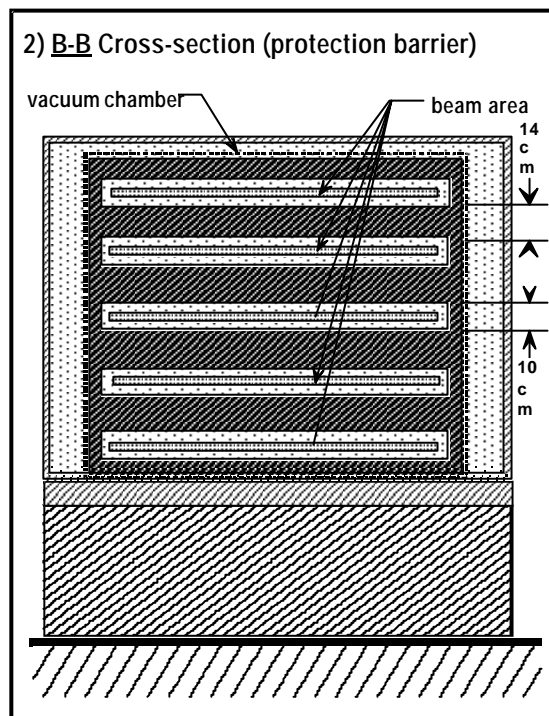
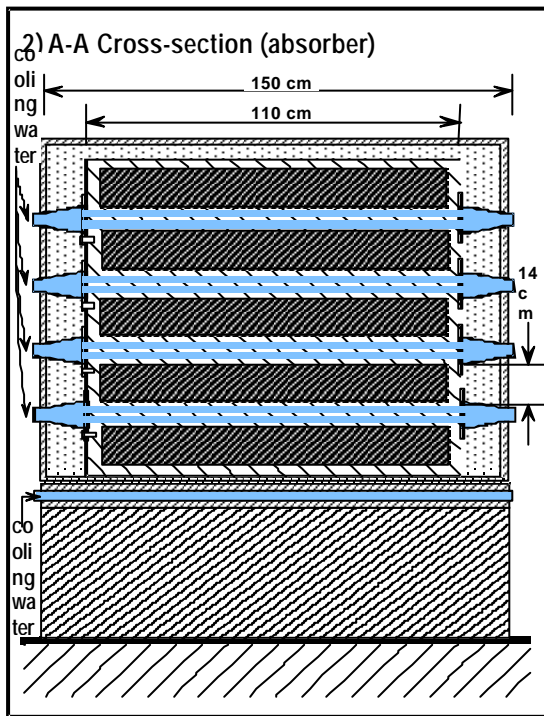
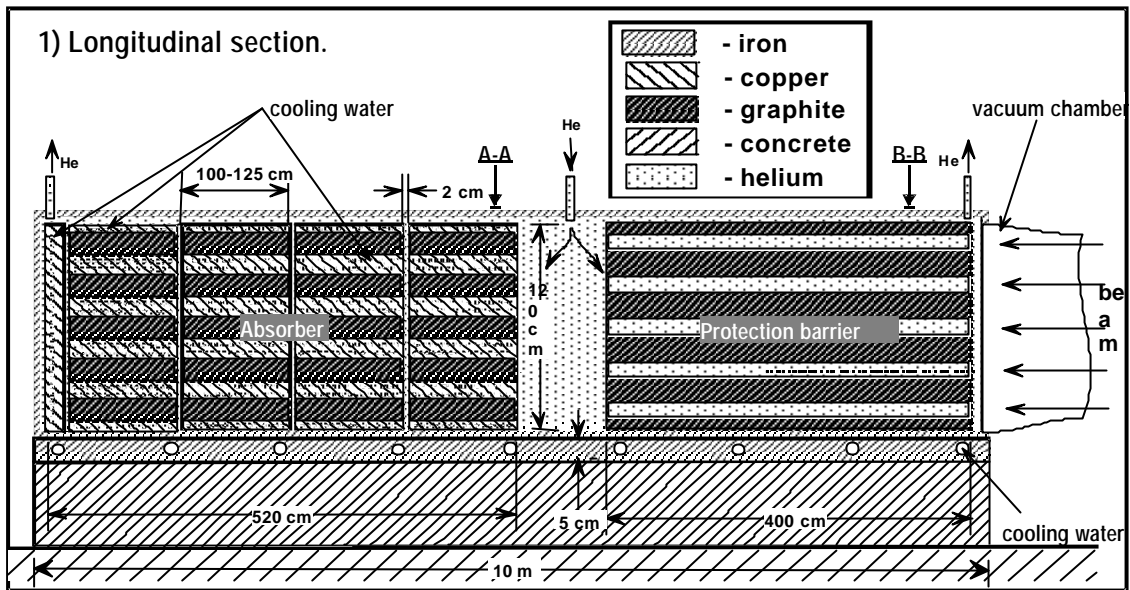


Figure 1: Schematic view on the graphite based solid dump scheme

3.1 Energy Deposition

For a beam with CDR parameters (see table 1) the maximum deposited energy density in graphite is 4.3 kJ/g per one bunch train passage. It corresponds to an instantaneous temperature jump in graphite of about 2500 K. In order to reduce this value, all particles of the bunch train are distributed on the face of the dump along a circular line with radius R by means of a fast sweeping system [6]. Figure 2 shows the maximum deposited energy density per one incident electron $(dE/dm)_{\max}$ on graphite as

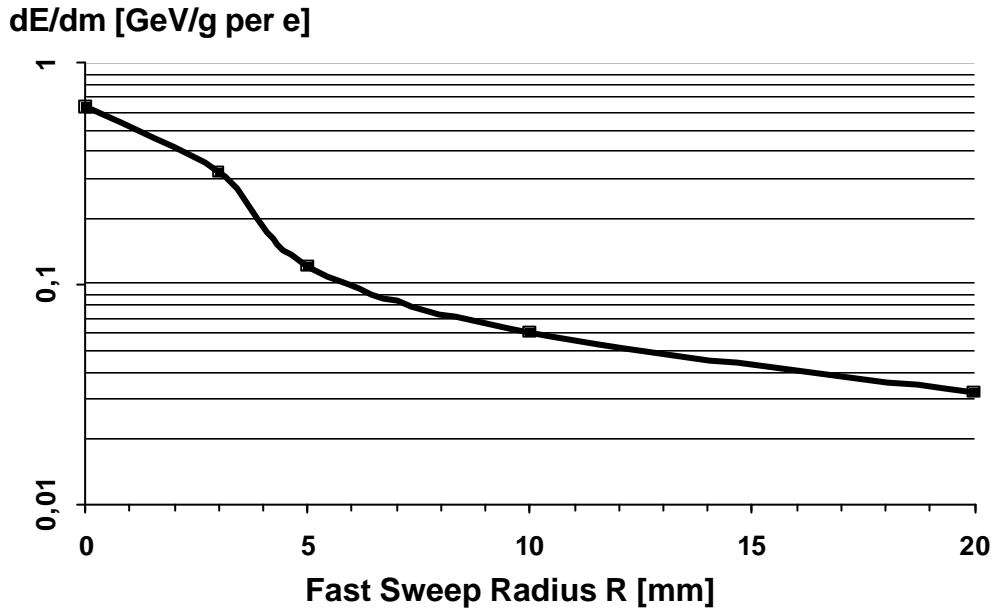


Figure 2: Maximum energy density per one incident particle $(dE/dm)_{\max}$ as a function of fast sweep radius R, 250 GeV electrons on water, $\sigma_x = 3\text{mm}$, $\sigma_y = 0.5\text{mm}$

a function of the fast sweep radius R. A sweep radius of 10mm is selected. Thus instantaneous heating is diminished about 10 times and temperatures in graphite are tolerable.

To estimate the direct power deposition into the cooling water, simulation runs were

| | Graphite | Copper | Cooling Water |
|---|----------|--------|---------------|
| Fraction of incident energy [%], deposited in ... | 91.5 | 6.5 | 0.03-0.1 |

Table 9: Fractional distribution of incident energy amongst the materials of the dump

made with a 1-2 cm thick water layer on the lateral surface of the dump block. Integrated absorbed energy in various sections of the dump is shown in table 9.

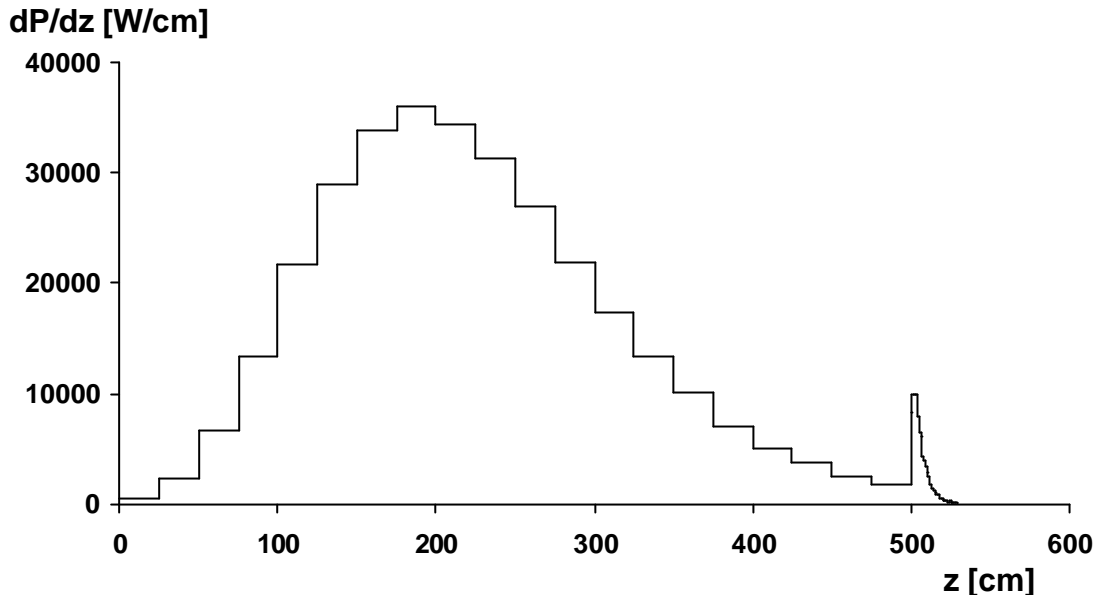


Figure 3: Longitudinal distribution of absorbed power dP/dz for the solid dump, distance between entrance window and Cu tail catcher is 500 cm

The longitudinal distribution of absorbed power in the graphite dump (dP/dz) is shown in figure 3. For the graphite section the maximum value of (dP/dz) is 36 kW/cm. The second peak at the end of the dump corresponds to the copper section (tail catcher), installed to decrease leakage energy from the dump. The spatial distribution of energy deposition density is used in section 3.3 on thermal and mechanical stress analysis. As will be shown there too, the peak temperature in graphite can reach about 800°C. At temperatures >500°C oxidation reactions occur in graphite. To avoid these processes, the dump must be enclosed by a container, which is filled with a noble gas (e.g. helium, argon or neon) at normal pressure.

3.2 Slow Sweeping System

Handling the problem of average heating in a solid dump, a large transverse cross section for heat conduction has to be established. Therefore the absorber needs to have large transverse dimensions while the incoming beam must be evenly distributed at its face along a line with length w . As shown in table 5 this slow sweep length will reach about 6m for a 11 MW beam hitting a graphite absorber. To provide this, a slow sweeping system is necessary. It consists of a pair of orthogonal dipoles. The first dipole is used to sweep the beam across the graphite block in horizontal plane. The second dipole transfers the beam to the next graphite plate in vertical direction. This must take place during the time gap between two bunch trains, i.e. ≈ 200 ms for TESLA. Assuming a pure drift space, the required peak deflecting angles are 10 mrad horizontally and 4×2.4 mrad vertically, if the dipoles are located 100 m upstream of the dump. For a 250 GeV beam this requires integrated field strengths of about 9 Tm and 4×2 Tm respectively.

To provide a homogeneous heat load, the total sweeping time must be significantly shorter (3-4 times) than the characteristic time of thermal diffusion in the dump. The thermal time constant can be estimated as 200-250 s. Therefore the full cycle of such a

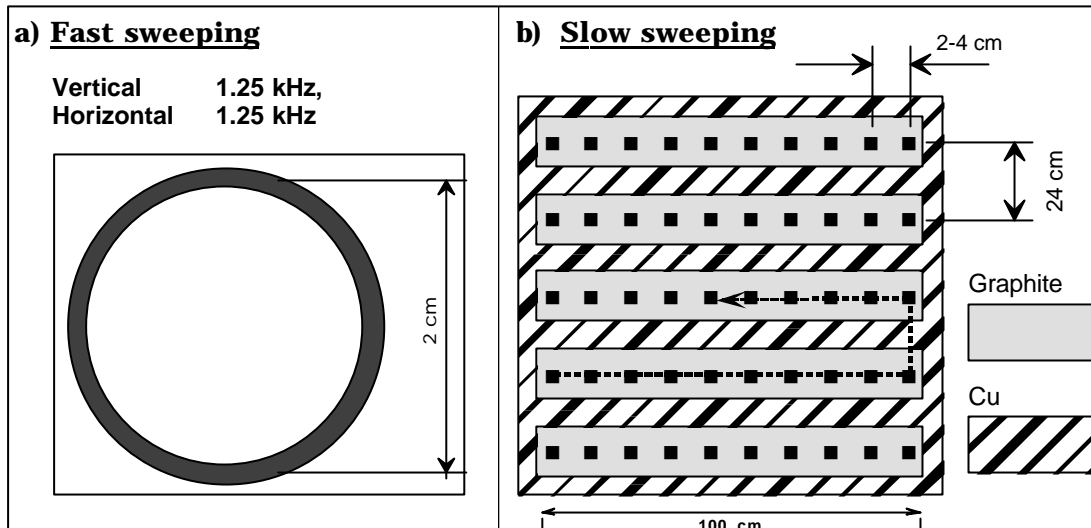


Figure 4a: Beam distribution at the dump face according to fast and slow sweeping

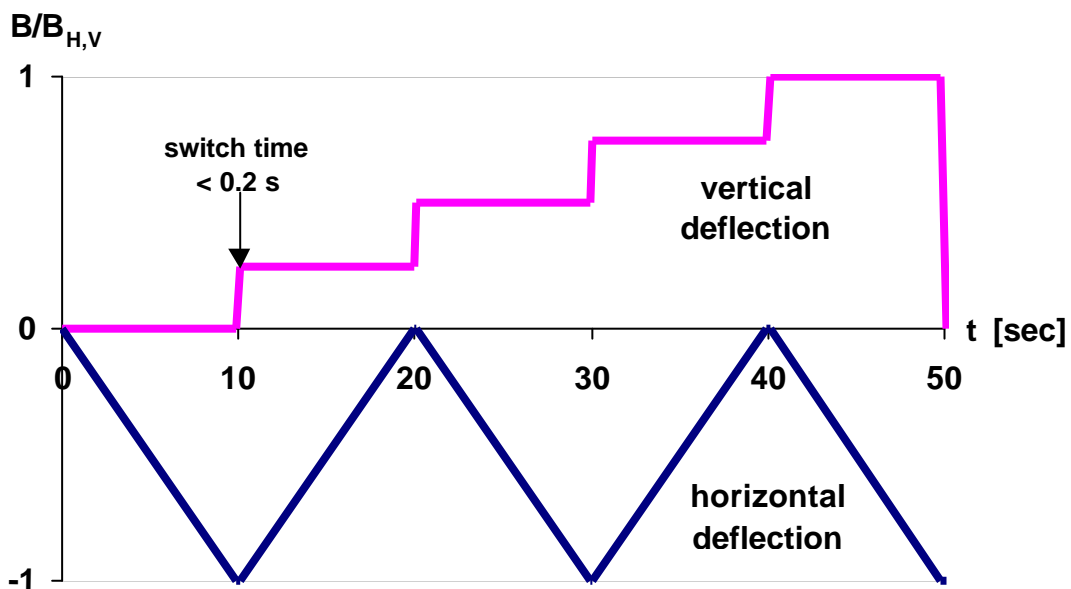


Figure 4b: Scheme of full deflection cycle of the slow sweeping system

slow sweeping system should be 50–80 s, or less. In this sense the attribute “slow” has to be understood in contrast to the fast sweeping system, where the beam distribution is done within the bunch train passage time of about 1 ms. In an overview figure 4a shows the beam distribution according to slow and fast sweeping systems. The time diagram of a full cycle of the slow sweeping system for the graphite dump is shown in figure 4b.

3.3 Thermal and Mechanical Stress Analysis of the Graphite based Solid Dump

On the basis of the CDR-type beam parameters from table 1, the ANSYS code [7] (version 4.4) has been used to calculate temperatures and mechanical stresses in the absorbing part of the dump. A cartesian coordinate system is chosen, where the z-axis directs along the depth of the absorber, while x- and y-axis give the horizontal

respectively vertical direction. For the calculations the absorber is longitudinally divided into 1.0-1.25 m long sections. All calculations were performed for one graphite-copper layer. The region around the shower maximum in graphite is the one of most interest and therefore especially focussed on.

The temperature jump at the graphite-copper boundary depends on its heat transfer coefficient K_{C-Cu} . The results of calculations are given for $K_{C-Cu} = 0.2 \text{ W/cm}^2/\text{K}$, which is close to the heat transfer coefficient at an Al-C boundary [8]. The cooling water temperature of the dump is 300 K. The graphite-copper section is cooled at both sides assuming $K_{Cu-Water} = 0.5 \text{ W/cm}^2/\text{K}$. Under these boundary conditions the maximum temperature in graphite reaches 980 K, i.e. $\approx 700^\circ\text{C}$. It is the sum of the instantaneous and equilibrium temperature rise which add to the temperature of the cooling water. The temperature jump on the graphite-copper boundary is 50 K.

Concerning mechanical stress analysis the components σ_x , σ_y , σ_z of the stress field were determined. Differences between them are important for estimation of the tolerable value of a heat stress. In terms of equivalent stress, safe operation of the dump has to obey the following criterion:

$$\sigma_e = \sqrt{\left((\sigma_x - \sigma_y)^2 + (\sigma_x - \sigma_z)^2 + (\sigma_y - \sigma_z)^2 \right) / 2} \leq \sigma_{\text{tolerable}}$$

The following two cases were considered:

Case 1: Stress calculation for the equilibrium temperature distribution

Case 2: Stress calculation for the equilibrium temperature distribution plus one TESLA train passage

To reduce the stresses as initiated by thermal expansion, the graphite section is cut into graphite sub-blocks of 5cm x 5cm x 24cm. The maximum stresses according to the calculations are:

| | |
|--------------------------------|-------------------------------|
| in case 1: | in case 2: |
| $\sigma_e = 11.3 \text{ MPa}$ | $\sigma_e = 18.7 \text{ MPa}$ |
| $\sigma_x = -8.1 \text{ MPa}$ | |
| $\sigma_y = -11.8 \text{ MPa}$ | |
| $\sigma_z = -10.5 \text{ MPa}$ | |

Negative values indicate compression. The maximum of the equilibrium stresses in graphite does not exceed 11.3 MPa. On top of this the cyclic stress will act with an amplitude of 7.4 MPa. The tolerable cyclic compression and tension stresses for standard reactor graphite at 1000 K are 55 MPa and 26 MPa respectively. Therefore this graphite meets the thermal and mechanical requirements for operation in the dump core of the solid dump scheme.

3.4 Water Cooling

Average power deposited by the electromagnetic shower in the graphite copper sections has to be removed by transverse heat conduction towards the water pipes. Since this heat flow depends on the longitudinal position, five 1m long intervals are considered.

| | z = 0-1 m | z = 1-2 m | z = 2-3 m | z = 3-4 m | z = 4-5 m | Cu tail catcher z > 5m |
|--|--------------|--------------|--------------|--------------|--------------|---------------------------|
| P_{abs} [MW] $\Sigma=8$ MW | 0.568 | 3.02 | 2.96 | 1.11 | 0.321 | 0.0816 |
| $P_{\text{abs}} / 8\text{MW}$ [%] | 7.05 | 37.4 | 36.7 | 13.7 | 4.05 | 1 |
| q_{ave} [W/cm^2] | 5.7 | 30.2 | 29.6 | 11.1 | 3.2 | |
| V [l/s] $\Sigma=72$ l/s | 5 | 27.3 | 26 | 10 | 3 | 0.7 |
| $K_{\text{Cu-Water}}$ [$\text{W}/\text{cm}^2/\text{K}$] for $\Delta T=50\text{K}$ | 0.12 | 0.64 | 0.49 | 0.22 | 0.06 | |

Table 10: The beam dump cooling system data

where:

| | |
|-----------------------|--|
| P_{abs} | absorbed power |
| q_{ave} | average transverse heat flux per unit of area |
| V | volume flow of cooling water to provide heat removal, assuming a temperature difference of 30 K between in- and outlet temperature |
| $K_{\text{Cu-Water}}$ | required heat exchange coefficient at the Cu-Water boundary, to keep the temperature jump there ≤ 50 K |

For each of these longitudinal intervals table 10 shows the situation in terms of the relevant parameters.

3.5 Summary of Solid Dump Characteristics

As a result of the calculations made in the previous sections, the characteristics of the graphite based solid beam dump are presented in table 11.

| | |
|---|------------------------|
| overall cross section | 150 cm x 150 cm |
| total dump length | 10 m |
| absorbing dump part | 5.2 m |
| protection section length (graphite collimator) | 4 m |
| total dump weight | 40 tons |
| total copper volume | 2.5 – 3 m ³ |
| total graphite volume | 6.5 m ³ |
| Graphite-copper section: Length | 1.0 - 1.25 m |
| Graphite-copper section: Cross section | 24 cm x 120 cm |
| Number of sections | 5 |
| required beam size at dump face without fast sweeping | $\sigma \geq 6$ mm |
| fast sweep radius R for beam size $\sigma_x \times \sigma_y = 3\text{mm} \times 0.5\text{mm}$ | 10 mm |
| slow sweep pathlength | ≈ 6 m |
| entrance window size | 1 m x 1 m |
| cooling-Water flow rate | > 72 l/s |

Table 11: Main parameters of the solid dump

4 Concept of the Water based Beam Dump

The following sections discuss an abort system scheme, which is based on a liquid absorber material, namely water. All numbers, data and considerations presented in the subsequent sections are based on the TDR parameters for the 250 GeV TESLA main linac, as given in table 1. The water beam dump system can be divided up into to main subsystems, the water absorber itself and the water cooling resp. preparation system.

4.1 The Water Absorber

The water beam absorber for the TESLA main beam abort system is a cylindrical vessel with an entrance window at both sides. It is 10 m long, 120 cm in diameter and contains about 10 m³ of water. For its corrosion resistance and mechanical strength titanium is considered as a candidate for the vessel material. In that case the walls need to be 15 mm thick. Its corrosion velocity is ten times less than that for stainless steel.

The water tank is equipped with two 200 mm diameter beam entrance windows from both sides [9]. On one side the spent beam can enter the absorber, while the other side is used as an entrance for the emergency extraction line.

Removal of the heat as continuously generated by the 12 MW beam is provided by means of water circulation towards an external heat exchanger. At a temperature drop of 30 K between in- and outlet, the required water flow rate is 100 kg/s.

To avoid accumulation of instantaneous heat, the cooling water is injected in the vessel through water inlet holes, which are equally distributed along the vessel length. To renew the water volume in the central part of the shower between successive bunch trains, a water velocity at the beam axis of not less than 50 cm/s has to be established.

A gas filled volume of 1000 liters at the top part of the tank is foreseen to compensate for slow water volume changes due to thermal expansion. In addition this gas buffer may help to protect the vessel from fast transient pressure waves, which is still under investigation.

4.1.1 Energy deposition and energy leakage

For a cylindrical water absorber, which is hit by a 250 GeV or 400 GeV electron beam, the percentage of energy leaking from it radially and longitudinally is given in

| Energy | $r_{\text{norm}} = 30 \text{ g/cm}^2$ | $r_{\text{norm}} = 50 \text{ g/cm}^2$ | $r_{\text{norm}} = 60 \text{ g/cm}^2$ | $r_{\text{norm}} = 70 \text{ g/cm}^2$ |
|---------|---------------------------------------|---------------------------------------|---------------------------------------|---------------------------------------|
| 400 GeV | 3.3 % | 1.3 % | 0.75 % | 0.55 % |
| 250 GeV | 3.3 % | 1.3 % | 0.80 % | 0.56 % |

Table 12: Fractional energy leakage from a cylindrical water absorber versus its normalized radius r_{norm} , ($l_{\text{norm}} = 3000 \text{ g/cm}^2$).

| Energy | $l_{\text{norm}} = 500 \text{ g/cm}^2$ | $l_{\text{norm}} = 700 \text{ g/cm}^2$ | $l_{\text{norm}} = 800 \text{ g/cm}^2$ | $l_{\text{norm}} = 900 \text{ g/cm}^2$ |
|---------|--|--|--|--|
| 400 GeV | 16 % | 2.2 % | 0.70 % | 0.23 % |
| 250 GeV | 13 % | 1.6 % | 0.52 % | 0.18 % |

Table 13: Fractional energy leakage from a cylindrical water absorber versus its normalized length l_{norm} , ($r_{\text{norm}} = 2000 \text{ g/cm}^2$).

| | | Neutrons | Charged Hadrons | Electrons and Positrons | Photons | Muons |
|------------------------|-----------|----------|-----------------|-------------------------|---------|---------|
| # of leaking particles | Radially | 1.3 | 0.23 | 13.3 | 610 | 0.01 |
| | Backwards | 0.01 | 0.0003 | 0.006 | 0.04 | 0.00015 |
| | Forwards | 0.01 | 0.003 | 2 | 20.6 | 0.002 |
| | Total | 1.32 | 0.23 | 15.5 | 630.6 | 0.013 |
| Leakage energy [GeV] | | 0.2 | | 0.15 | 1.6 | 0.013 |

Table 14: Number of particles and their energy as leaking through the different surfaces of a water cylinder (10m long, 120cm in diameter), results are normalized to one incoming 250 GeV electron.

table 12 and table 13. To be independent of the water expansion due to temperature, the data is given as a function of the normalized radius $r_{\text{norm}} = r/\rho$ and the normalized length $l_{\text{norm}} = l/\rho$. Assuming a 1 % total energy leakage limit, table 12 and table 13 require an absorber with a length of not less than 750-800 g/cm² and a radius not less than 52-55 g/cm². Therefore a water cylinder with 60 cm in radius and 10 m of length is considered. The number of secondary shower particles and their energy as leaking through the different surfaces of such a water volume is listed in table 14. All results are normalized to one incoming 250 GeV electron.

Dominated by radial leakage the total amount does not exceed the 1% level, but in absolute numbers this is still 120 kW, which will heat the shielding, by which the water dump has to be tightly enclosed, up to intolerable temperatures if concrete is used. For its low residual radioactivity and high thermal conductivity a removable inner shell of aluminium, thermally coupled to the dump vessel is proposed [10] to reduce the power density before concrete is employed more outside. Gaps between vessel and shield or within the shielding volume have to be strictly minimized in order to limit air activation.

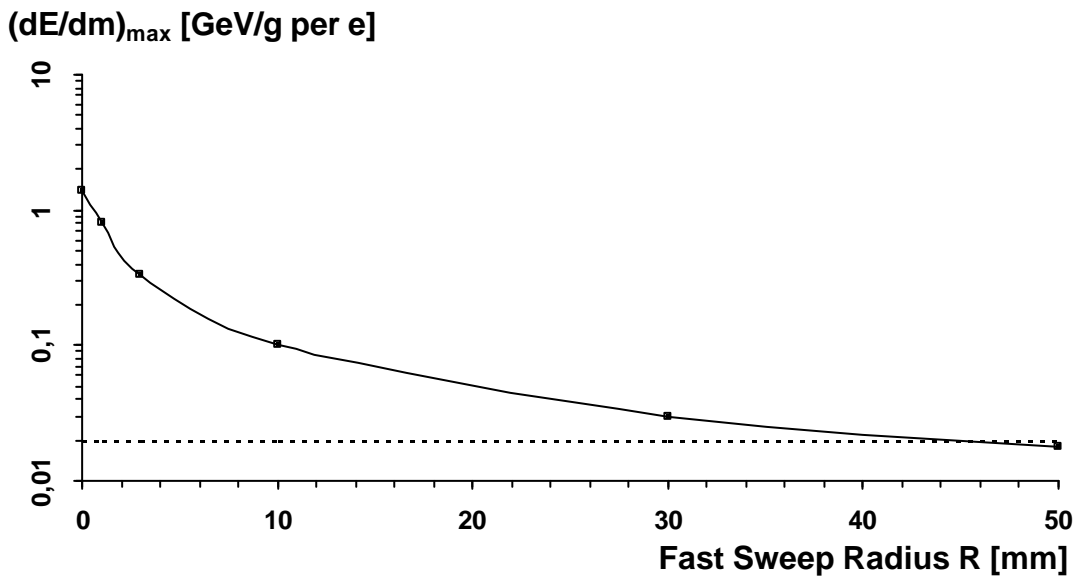


Figure 5: Maximum energy density in water $(dE/dm)_{\text{max}}$ per one 250 GeV incident electron as a function of fast sweep radius R

Similar to the solid dump scheme a fast sweeping system [6] is required for the water dump as well, in order to keep instantaneous heating of the water during one bunch train passage below a safe limit of about $\Delta T_{\text{inst}} \leq 40\text{K}$. All bunches of the bunch train are distributed along a circle of radius R at the dump face. The maximum energy deposition $(dE/dm)_{\text{max}}$ per one incident 250 GeV particle as a function of the fast sweep radius is shown in figure 5. For $N_t = 5.64 \cdot 10^{13}$ particles per bunch train the 40 K limit is reached at about $dE/dm = 0.02\text{GeV/g}$ as indicated by the dashed line in figure 5. Thus a fast sweep radius of $R = 50\text{ mm}$ is required in that situation.

4.2 Water Cooling and Preparation System

As already mentioned above, the heat as dissipated in the absorber vessel will be removed by a continuous flow of vessel water towards an external heat exchanger. This one is part of a quite ambitious water preparation plant as shown in figure 6. Besides cooling it will also handle the radiological and hydrochemical aspects of the dump water. For this reason a two loop cooling system is considered.

Heat removal of 12 MW at a temperature drop of 30 K between in- and outlet

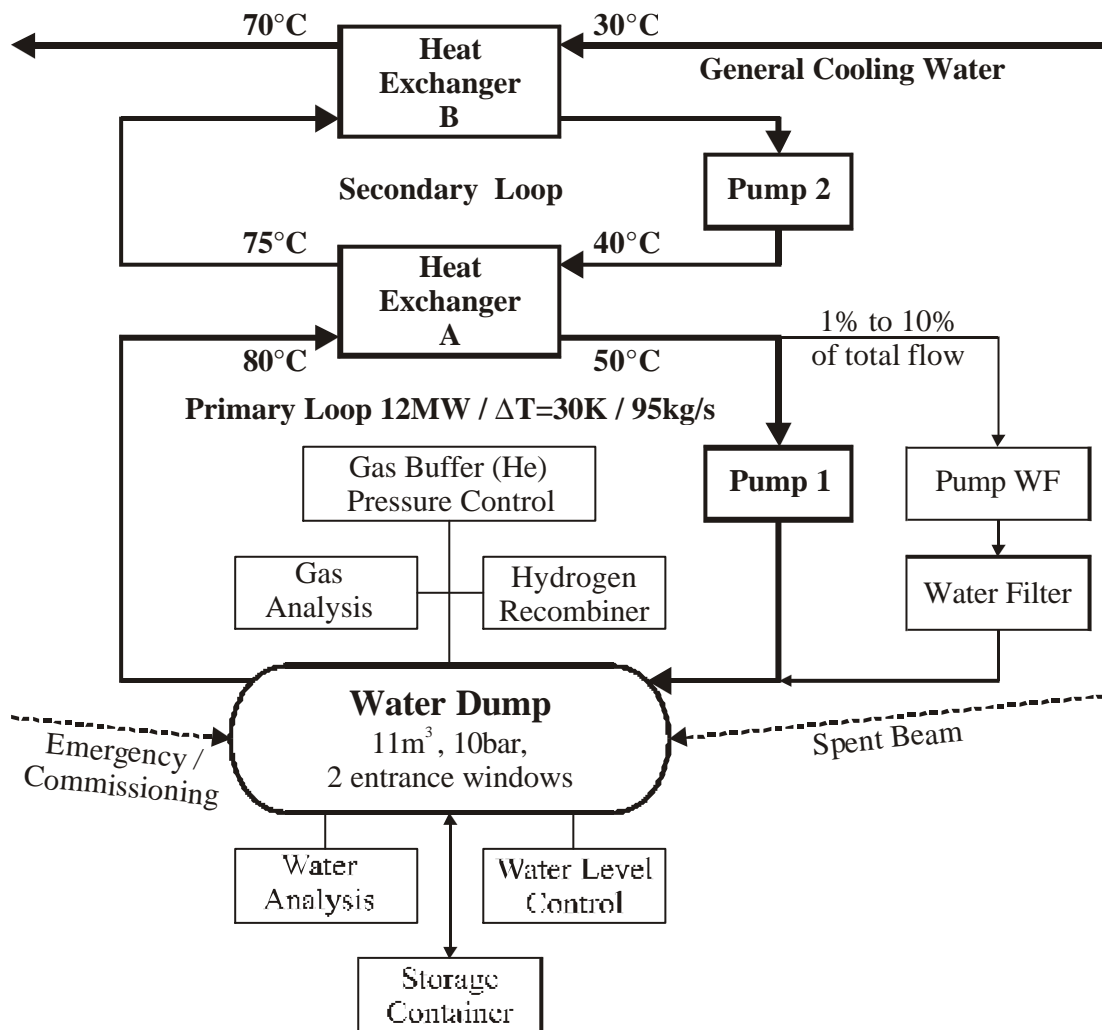


Figure 6: Scheme of the water system for the water based beam dump

requires a water flow rate of about $100\text{l/s} \Leftrightarrow 360\text{m}^3/\text{h}$. The primary loop will be filled only once and the water will stay there over the entire life of the collider. Besides the production of radioactive nuclei, which are extracted in a resin filter, the water is also affected by radiolysis. Therefore hydrogen is produced and has to be catalytically recombined. Obviously this system needs to be extremely gas- and leak-tight to a level as valid for vacuum systems. This requires gas-tight components (pumps, heat exchangers, ...), welded or metal sealed connections and a proper choice of materials in combination with the knowledge about the parameters defining hydrochemical processes.

However the possibility of leakage and therefore exchange of components has to be included in the concept. Having recognized such a failure by monitoring pressure and level of the water, the system can be emptied into the storage container. Thus maintenance work is simplified, because the biggest source of dose rate is taken away. All walls of the rooms dedicated for this system have to be sealed with a special paint to collect leaking water. Separation of the primary cooling circuit from the general cooling water by an intermediate secondary loop, operating at a higher static pressure than the primary one, protects the general cooling water from being contaminated even if both heat exchangers A and B have an internal leak simultaneously.

The main aspects of the primary water loop are presented in more detail in the following sections.

4.2.1 Working temperature and pressure

The in- and outlet temperatures of water in the cooling loops are shown in figure 6. The average temperature of the dump water is 65°C . As limited by fast beam sweeping, the maximum instantaneous temperature jump in water after one bunch train passage is 40 K. To prevent boiling of the dump water it is pressurized to 10^6 Pa (10 bar). The water boiling point at this pressure is 180°C . Therefore the temperature safety margin is 75K. Note that due to the total thermal capacity of the dump water, its average temperature rises by less than 0.5K during one bunch train passage with $N_t = 5.64 \cdot 10^{13}$ particles.

The static pressure is maintained by a gas buffer (most probably He), which is foreseen at the top of the dump vessel, to protect it from pressure waves induced by instantaneous heating in a failure case of the fast sweeping system. The gas buffer will as well compensate for volume change of the primary cooling water due to thermal expansion. Natural recombination of hydrogen will also profit from the higher pressure of the water.

The heat exchanger A of tube in tube type requires a heat exchange surface of about 1000 m^2 . Its cylindrical size is similar to that of the dump vessel.

4.2.2 Water radiolysis

The impact of high energy electrons absorbed in water leads to the production of hydrogen and oxygen by radiolysis. Besides the incident beam power the production rate depends on several parameters of the water, like its temperature, pressure, acidity (pH value) [11] and other conditions. At pH=3-4 the production is three to four times higher than in water with pH=6-7. Starting with water of pH=7-8 hydrogen production is more or less independent of the hydrogen concentration. There are data, which indicate, that hydrogen production can be suppressed by introducing small additives of

such substances as ammonia, hydrazine or alcohol (C₂H₅OH). This question requires additional experimental study.

Hydrogen production rate in water measured at normal conditions is 0.3 liter per MJ of energy absorbed in water [12]. According this data for 12 MW average absorbed beam power in water the hydrogen production rate is 3.6 l/s. Gas solubility in water is limited and radiolysis gases will accumulate in the gas volume at the top of the absorber. The explosive limit of hydrogen concentration in air is 4%. Therefore a noble gas is required for the gas buffer. H₂ and O₂ have to be recombined catalytically in a Pd-Pt hydrogen recombiner. Even if the equilibrium hydrogen concentration due to other effects of recombination would be already tolerable, a catalytic recombiner is heavily required in a case of a pressure release and thus outgassing of the water.

4.2.3 Radioactivity and water filtering

Radioactivity in pure water is produced via photon-nucleus and hadron-nucleus interactions with the ¹⁶O water component. Besides shortlived radioactive nuclei (half-life in brackets) like ¹⁵O(2minutes), ¹³N(10minutes), and ¹¹C(20minutes) also ⁷Be(53.6days) and ³H(12.3years) are produced in pure water. At continuous 12MW operation the activity of the latter two candidates saturates at about 60 TBq for ⁷Be and at 146 TBq in the case of ³H [13]. After decay of the shortlived ones and since the 20 keV electrons from tritium decay will not penetrate the walls of the water system, the outside dose rate is mainly determined by 478 keV gamma rays from ⁷Be decay. If evenly distributed in a total water volume of 10 m³, the estimated dose rate at the surface of a 300mm diameter pipe is about 500mSv/h.

Note that these considerations assume pure water. Other products coming from corrosion of the water system will be dissolved in the dump water as well. They represent an additional source of radioactive nuclide production. To reduce the concentration of nuclides in the water, a water filter is introduced. A certain fraction β (typically 1-10%) of the total water mass flow dm/dt is directed into a filter line. For a total water inventory of mass M the saturation concentration of a radioactive nuclei with a half life of t_{1/2} = ln 2 · τ is reduced by the following factor F due to the presence of the filter:

$$F = 1 + \varepsilon \cdot \beta \cdot \tau \cdot \frac{dm/dt}{M}$$

where ε is the extraction efficiency of the filter for the element under consideration. For M=10⁴kg, dm/dt=100kg/s and ε · β = 1% – 10% the saturation concentration of ⁷Be is reduced by two to three orders of magnitude.

Typically appearing as ??? molecules dissolved in water, tritium (T) can not be removed by simple filtration. Therefore the whole system must be leak-tight as mentioned previously.

4.3 Summary of Water Dump Characteristics

As a result of the considerations made in the previous sections, the characteristics of the water based beam dump are presented in table 15.

| | |
|---|---|
| Absorber Vessel | |
| total length | 10 m |
| cross section | 1.2m in diameter |
| weight | 3000 kg for Ti tank 5000 kg for stainless steel option |
| Primary Loop | |
| total volume | 15 m ³ |
| absorber volume | 11 m ³ |
| gas buffer volume | 1-1.5 m ³ |
| static pressure | 10 bar |
| average working temperature | 65°C |
| cooling water mass flow | 100 kg/s (12MW, $\Delta T=30K$) |
| transverse water velocity in the region of the shower maximum | ≥ 0.5 m/s |
| Fast Sweeping System | |
| required beam size without fast sweep | $\sigma \geq 19$ mm |
| fast sweep radius for $\sigma_x \times \sigma_y = 1\text{mm} \times 0.4\text{mm}$ | ≥ 50 mm |
| frequency | ≥ 1 kHz |

Table 15: Main parameters of the water dump

5 Conclusion

For a huge amount of average beam power in the 10 MW-regime heat removal efficiency defines the power capability of a beam absorber. Due to limited heat conductivity the graphite based solid beam dump scheme needs a rather complicated system of heat sinks incorporated into carbon enabling a large surface of heat exchange. Therefore slow beam sweeping along a large path length of about 10 m and consequently a huge exit / entrance window (about 1m diameter) are required. In addition the whole 40 tons absorber must be enclosed by a containment, which is filled with noble gas to prevent graphite oxidation. There is no doubt that the technical solution of a solid absorber scheme will result in an extremely complicated design in terms of manufacturing and maintainance. Thus a reliable long term operation can be excluded.

In contrast to that a water absorber scheme offers much more flexibility in terms of handling and maintainance. In addition it can be easily adjusted for different power capabilities by adjusting the water mass flow. The size of the absorber is purely defined by shower containment constraints instead of heat conduction. Slow beam sweeping is not necessary. Since dealing with an activated water system a safe and careful technical design of this facility is a challenging task which requires highest priority. However, similar water systems, from which technical experience can be derived, are already in use at spallation neutron sources or research reactors.

Therefore the only reasonable and technically feasible solution for a high power beam dump beyond several hundreds of kW is a water based scheme.

6 References

- [1] R. Brinkmann, Basic Assumptions for the TESLA TDR, DESY, April 2000
- [2] Review of Particle Physics, Phys. Rev., D54,1 (1966)
- [3] N. V. Mokhov, The MARS Code System User's Guide, Version~13(95)'', Fermilab-FN-628 (1995),
N. V. Mokhov et al., Fermilab-Conf-98/379 (1998),
<http://www-ap.fnal.gov/MARS/>
- [4] Conceptual Design of a 500 GeV e^+e^- Linear Collider with integrated X-ray Laser Facility, DESY 1997-048, p 512
- [5] Structural Material, Handbook, Mashinostroenie, Moscow,1990
- [6] V. Sytchev et al., Concept of the Fast Beam Sweeping for the e^\pm Beam Dumps of TESLA, DESY February 2001, TESLA-Report 2001-05
- [7] ANSYS, User Manual, Swenson Analysis Systems Inc., (1983)
- [8] J. Kidd et al., A High Intensity Beam Dump for the Tevatron Beam Abort System, PAC IX, Washington, 1981
- [9] M. Maslov et al., Concept of Beam Entrance and Exit Windows for the TESLA Water based Beam Dumps and its related Beam Lines, DESY, February 2001, TESLA Report 2001-07
- [10] D. Dworak, J. Loskiewicz, Direct Energy Deposition in the Lateral Concrete Shielding of the TESLA Water Dump and the Rise of Shielding Temperature, Report No. 1854 / PH, The Henryk Niewodniczanski Institute of Nuclear Physics (HNINP), Kraków, Poland, November 2000
- [11] V. Byakov, F. Nichiporov, Water Radiolysis in Nuclear Reactors, Moskow, Energoatomizdat, 1990
- [12] D. R. Walz, E. J. Seppi, Radiolysis and Hydrogen Evolution in the A-Beam Dump Radioactive Water System, SLAC-TN-67-29, October 1967
- [13] TESLA Technical Design Report (TDR), see chapter on radiation safety (8.3.6), DESY March 2001,